

Observation of Plasma Heating Due to Parametric Instabilities at the Upper Hybrid and at the Cyclotron Harmonic Frequencies*

B. Grek and M. Porkolab

Plasma Physics Laboratory, Princeton University, Princeton, New Jersey 08540

(Received 18 December 1972)

Strong plasma heating is observed in external electric fields near the upper hybrid frequency or near the electron cyclotron harmonics. It is shown that the fast plasma heating is associated with the presence of the parametric instability of Bernstein waves, ion-acoustic waves, and lower hybrid waves.

The microwave irradiation of plasmas near (or above) the electron cyclotron frequency (i.e., its harmonics, or at the upper hybrid frequency) is used extensively for heating plasmas. It is usually assumed that such heating is due to¹⁻⁵ (a) electron cyclotron resonance heating at $\omega = \omega_{ce}$; (b) linear mode conversion at the upper hybrid frequency ($\omega > \omega_{ce}$) and subsequent absorption by linear dissipation mechanisms; (c) heating by stochastic processes assuming multimode field distributions. In this Letter we present experimental results which show that in sufficiently strong rf fields very efficient plasma heating may occur above the electron cyclotron frequency through excitation of the parametric decay instability of electrostatic cyclotron harmonic waves (Bernstein waves) and ion-acoustic waves which propagate almost perpendicularly to the magnetic field.⁶ In addition, parametric decay into Bernstein waves and lower hybrid waves is also observed.^{7,8} However, in this case we find that the saturated spectrum remains sharply spiked, and the heating is less than in the case of decay into the broad, turbulent ion-acoustic spectrum. Efficient heating is observed when the frequency of the external field is near or just above the upper hybrid frequency, or at harmonics of the electron cyclotron frequency. Thus, in these cases the external field is in the accessible regime for the extraordinary mode, so that the whole plasma column may be penetrated by the rf fields. No linearly excited electrostatic wave is observed at the pump frequency, and the heating occurs *only* above the threshold rf power for the foregoing parametric instability. The measured heating times are orders of magnitude faster than linear dissipation mechanisms would predict.

The experimental apparatus has been described previously.⁶ The experimental parameters were as follows: $0.1 \lesssim \omega_{pe}^2/\omega_{ce}^2 \lesssim 2$, He gas, $T_{e0} = 3$ to 7 eV, $T_{ie} \lesssim 0.1$ eV, pump frequency $f_0 = 0.3 - 1.0$

GHz, and electron collision frequency $\nu_{e0}/\omega_0 \lesssim 10^{-3}$. The electric field was applied perpendicularly to the magnetic field between two grids, which were fed by a wide-band balanced transformer. Wavelength and frequency measurements were carried out by means of shielded high-frequency probes which were movable radially or axially.⁶

Figure 1 shows examples of the decay spectrum for pump field strengths above threshold, and their location on the Bernstein-wave dispersion curves.^{7,9} The low-frequency components of the spectrum (not shown here) satisfied the usual frequency (energy) selection rules.⁶ The wavelengths of the waves were measured with an interferometer which included two double-conversion superheterodyne narrow band-pass ($\Delta f \approx 30$ kHz) receivers.⁶ The following decay processes were identified in the present experiments: (i) Decay into lower hybrid waves and Bernstein (or upper hybrid) waves.^{7,8} In particular, the measured parallel wavelengths of the lower hybrid waves were of the order of 100 cm, which gave parallel phase velocities larger than the thermal velocity of the electrons. The dispersion relation was verified by measuring the perpendicular wavelengths and checking their dependence on ion mass, magnetic field, and density.⁷ The perpendicular wave numbers of the Bernstein waves were found to be the same as that of the lower hybrid waves, thus confirming the usual wave-vector selection rules ($k_0 = 0$).⁹ (ii) Decay into ion-acoustic waves and Bernstein waves. Contrary to the lower hybrid waves, the perpendicular ion acoustic wavelengths were independent of the magnetic field and density, and the measured parallel wavelengths (of the order of 5 cm) gave $\omega/k_{||}v_{te} < 1$ as expected.⁷ Although we have previously reported the parametric decay instability of Bernstein waves and ion-acoustic waves, in those experiments we had $\omega_{pe}^2/\omega_{ce}^2 > 1$, $\omega_0 \ll \omega_{UH}$ (where ω_{UH} is the upper hybrid

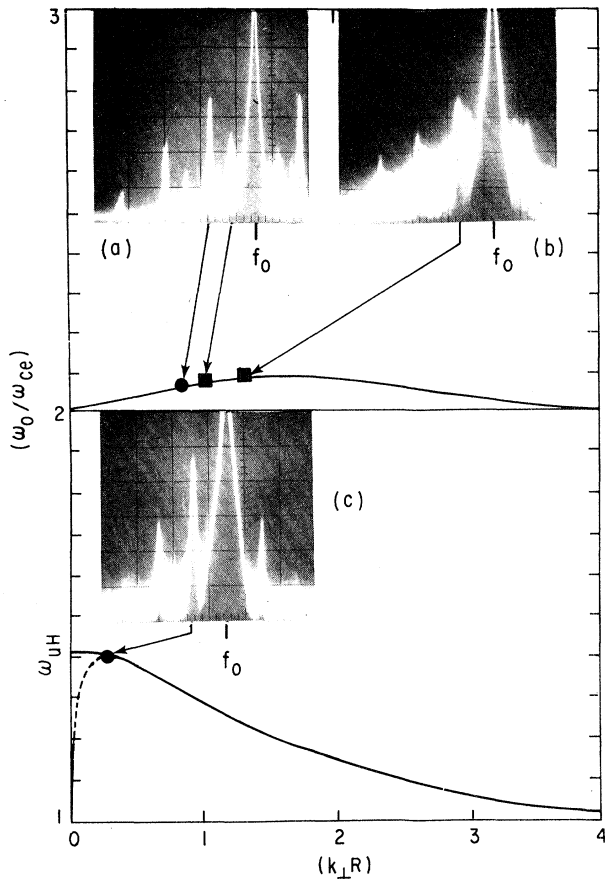


FIG. 1. Dispersion relation for Bernstein waves for $\omega_p = \omega_c$. R is the electron Larmor radius; the dotted line shows effects of finite k_{\parallel} . Insets (a) to (c) show typical decay spectra. The dots are associated with decay into lower hybrid waves, and the squares with ion-acoustic waves. $\omega_0/\omega_c = 2.12$ for spectrum (a), 2.08 for (b), and 1.50 for (c).

frequency) so that the pump field (ω_0) was always evanescent.⁶ In contrast to the present results, no substantial heating was observed in the main body of the plasma column. In both cases (i) and (ii) we found that for decay wavelengths short compared with the grid spacing (6–8 cm), both the measured thresholds and growth rates agreed well with linear theory.⁹

For a given value of $\omega_{pe}^2/\omega_{ce}^2$ the two types of decay processes may occur simultaneously or separately, depending on the exact values of ω_0/ω_{ce} . In particular, in Fig. 1, spectrum (a), decay into both ion-acoustic waves and lower hybrid waves is occurring. In spectrum (b) the Bernstein waves couple with ion-acoustic waves only. In spectrum (c) the Bernstein waves couple with lower hybrid waves only. In order to decide

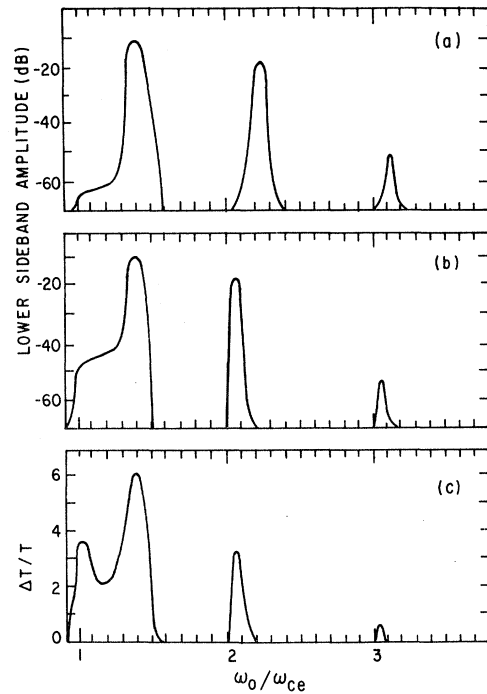


FIG. 2. (a) Amplitudes of Bernstein waves which couple with lower hybrid waves; $\omega_{ce} = \omega_{pe}$; ω_0 (the pump frequency) is varied. (b) Amplitudes of Bernstein waves which couple with ion-acoustic waves. (c) Fractional increase of the main electron body temperature as obtained from a swept Langmuir probe; $P_0 \approx 30$ W.

which process was occurring, it was necessary in each case to determine whether the parallel phase velocity was less or greater than the electron thermal velocity.⁷ A large number of such measurements were made in the first three cyclotron harmonic bands, and a summary is given in Figs. 2(a) and 2(b). In particular, in Fig. 2(a) we show the variation of the Bernstein wave (lower sideband) amplitudes at high input rf power ($P_{in} \approx 30$ W) as a function of the pump frequency ω_0 . This figure is associated with the decay of the electromagnetic pump field into Bernstein waves and lower hybrid waves. Figure 2(b) shows similar results for the decay of the electromagnetic pump field into Bernstein waves and ion-acoustic waves. The amplitudes of the low-frequency waves (i.e., ion-acoustic waves and/or lower hybrid waves) varied with the pump frequency in a similar way to the amplitudes of Bernstein waves. Figure 2(c) shows the concomitant increase in the main electron body temperature as the pump frequency is varied. Plasma heating was measured by fast-sweep Langmuir probes ($T \approx 1 \mu\text{sec}$) and by a multigrid electrostatic energy analyzer.

In order to minimize the possible effects of the pump fields on the plasma heating measurements, the energy analyzer and probes were located from 20 to 60 cm from the interaction region. The rf power input into the plasma was constantly monitored to ensure that any field fluctuation inside the plasma was not due to changes in generator loading. In particular, below instability threshold ($P_0 \approx 0.5$ W) no plasma heating was observed. The maximum electron temperature (for the main body) was obtained near $\omega_0 \approx \omega_{UH} \approx 1.4\omega_{ce}$ (for $P_0 \approx 40$ W, $T_e \approx 30$ eV). We note a marked correspondence between the occurrence of the decay spectrum as predicted by the band structure of the linear dispersion relation⁹ (shown in Fig. 1) and the increase of the main electron body temperature as ω_0/ω_{ce} is varied. We see that near the cyclotron harmonic frequencies most of the heating is associated with the ion-acoustic wave decay. The smaller peak in $\Delta T/T$ at $\omega_0/\omega_{ce} \approx 1$ may be due to cyclotron resonance heating.¹⁻⁴ There is also some instability and heating in the regime $\omega_{ce} \lesssim \omega_0 \lesssim \omega_{UH}$ due to tunneling of the rf fields.⁷

The development of the electron distribution function, as measured by a multigrad energy analyzer, is shown in Fig. 3. Figure 3(a) shows the energy distribution function for different pump powers. For powers above, but less than 10 times instability threshold ($0.5 < P_0 < 5$ W) only the tail of the electron distribution function is heated. For powers greater than 10 times threshold the spectrum becomes turbulent and heating of the main body also takes place. Figure 3(b) shows the energy distribution for different times after the turn on of the pump. For short times ($T < 1$ μ sec) the tail of the electron distribution function is heated. For times $T > 1$ μ sec the main body of the electrons starts to heat and reaches its peak temperatures in about 2 μ sec. The main body temperature agrees with that measured with the fast-sweep Langmuir probe. At times later than 2 μ sec, the number of hot electrons decreases, whereas the main body temperature remains constant. Simultaneously, strong pump depletion is observed. We have also looked for ion heating, but did not observe any. This may be due to (i) strong interaction of the excited Bernstein waves (sidebands) with thermal electrons and fast pump depletion; (ii) too low magnetic field ($B \approx 100$ G) and hence fast ion loss. In particular, at the upper-hybrid frequency in the final state the self-consistent pump fields were reduced by about 20 to 75% from their in-

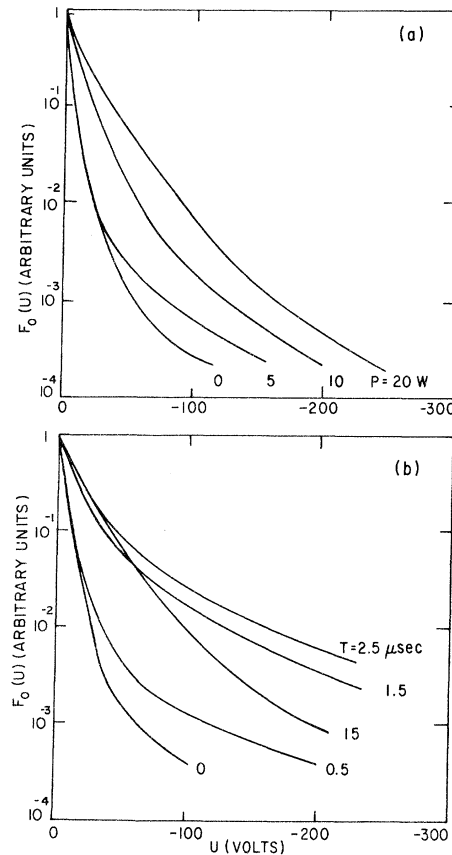


FIG. 3. (a) Electron energy distribution [$F_0(u)$] for different powers (P) 5 μ sec after the start of the heating pulse. $\omega_p/\omega_{ce} = 1$, $\omega_0/\omega_{ce} \approx 1.5$. (b) Energy distribution for different times (T) after the start of the heating pulse; $P_0 = 25$ W.

itial values (depending on experimental conditions). The peak amplitudes of the Bernstein waves attained 40 to 75% of the pump amplitude. The ion-density fluctuations were only $\tilde{n}/n_0 \approx 2$ to 5%. The number of hot electrons in the tail was 3 to 8% of that of the main body. For $\omega_0 \approx 2\omega_{ce}$ the peak wave fields were at most 15% of the pump field. The ion-density fluctuations were $\tilde{n}/n_0 \approx 1\%$, and the number of hot electrons in the tail was 1 to 5%.

In conclusion, we have reported experimental observation of fast heating of electrons by rf fields near the upper hybrid frequency and at the second and the third electron cyclotron harmonic frequencies. It was shown that a strong parametric decay instability occurred at the same time and it is believed to be responsible for the fast plasma heating observed. In particular, for maximum fields of the order of $E \approx 100$ V/cm,

the linear heating times estimated for the present experiment give $\Delta T_e \lesssim 1$ eV/ μ sec near the upper hybrid frequency. The enhancement at the second harmonic is many orders of magnitude smaller. Since our measurements show (see Fig. 3) that under these conditions $\Delta T_e \simeq 20$ – 30 eV/ μ sec, and that very energetic particles are also produced within a microsecond ($U \lesssim 500$ eV), it is clear that linear theories do not explain our results. We believe that similar processes may occur in a number of experiments where heating near the upper hybrid or the cyclotron harmonics have been observed.^{5, 10} In contrast to recent heating experiments with frequencies below the electron cyclotron frequency where mainly heating of the tail of the distribution function was observed,¹¹ in the present case considerable heating of the main body of electrons was also observed. This is believed to be due to the strong interaction of the excited Bernstein waves with thermal electrons. Thus, heating at frequencies above the electron-cyclotron frequency may be more favorable for possible applications where

fast heating of thermal electrons is desired.

*Work supported by the U. S. Atomic Energy Commission under Contract No. AT(11-1)-3073.

¹R. A. Dandl *et al.*, Nucl. Fusion **11**, 411 (1971).

²H. Ikegami, S. Aihara, and M. Hosokawa, Phys. Fluids **15**, 2054 (1972).

³J. C. Sprott, K. A. Connor, and J. L. Shohet, Plasma Phys. **14**, 269 (1972).

⁴O. Eldridge, Phys. Fluids **15**, 676 (1972).

⁵V. V. Alifkaev *et al.* Pis'ma Zh. Eksp. Teor. Fiz. **15**, 41 (1972) [JETP Lett. **15**, 27 (1972)].

⁶R. P. H. Chang, M. Porkolab, and B. Grek, Phys. Rev. Lett. **28**, 206 (1972).

⁷T. H. Stix, *Theory of Plasma Waves* (McGraw-Hill, New York, 1962), pp. 32, 41, 227, 244.

⁸S. Hiroe and H. Ikegami, Phys. Rev. Lett. **19**, 1414 (1967). Note that in this work the wavelengths were not measured, and the thresholds were not compared with theory.

⁹M. Porkolab, Nucl. Fusion **12**, 329 (1972).

¹⁰O. A. Anderson *et al.*, Bull. Amer. Phys. Soc. **17**, 997 (1972).

¹¹M. Porkolab, V. Arunasalam, and R. A. Ellis, Jr., Phys. Rev. Lett. **29**, 1438 (1972).

Rotation and Structure of Low-Frequency Oscillations inside the ST-Tokamak Plasma*

J. C. Hosea, F. C. Jobs, R. L. Hickok,† and A. N. Dellis‡

Plasma Physics Laboratory, Princeton University, Princeton, New Jersey 08540

(Received 26 February 1973)

Low-frequency oscillations, which can lead into the violent disruptive instability which sets the q (current) limit of tokamak operation, are investigated with a heavy-ion beam probe. Direct measurements of the space potential and the perturbation of the electron density *inside* the hot tokamak plasma resolve the electric field contribution to the mode rotation and the spatial structure of the mode.

The two phases of magnetohydrodynamic (MHD) instability observed in tokamaks^{1,2} appear jointly; low-frequency, low-amplitude oscillatory modes with helical magnetic field perturbations [$B_\theta \propto \exp(im\theta - i\varphi)$] are observed to grow leading into the more deleterious "disruptive" instability characterized by a negative spike on the plasma loop voltage (v_φ) and a partial depletion of the energy stored in the plasma (θ and φ are the minor and major azimuthal angles of the torus, respectively). As m decreases, the intensity of the disruptive instability increases, until following $m = 2$, the disruptive instability dominates the tokamak discharge. In fact, the $m = 2$ oscillations are observed to precede the violent disruptive instabilities at both the low

safety factor $q(a)$ and high-pressure (plasma density) limits to useful tokamak operation [$q(r) = rB_\varphi(R)/RB_\theta(r)$, where r and R are the minor and major toroidal radii, respectively, and a is the plasma limiter radius]. Apparently, the disruptive instability occurs when the radial current distribution $j_\varphi(r)$ is such that the $q = m$ singular magnetic surface location is favorable to the enhanced growth of the m -mode oscillation.¹ (Run-away electrons do not appear to cause the instability.³) When the $q = 2$ singular surface is moved toward the plasma surface by lowering $q(a)$ or by causing the current channel to shrink by increasing pressure as evidenced by a constriction of the electron temperature profile,^{1,4} the $m = 2$ mode grows to an amplitude of $\tilde{B}_\theta(d)/B_\theta(d) \sim 6\%$ at

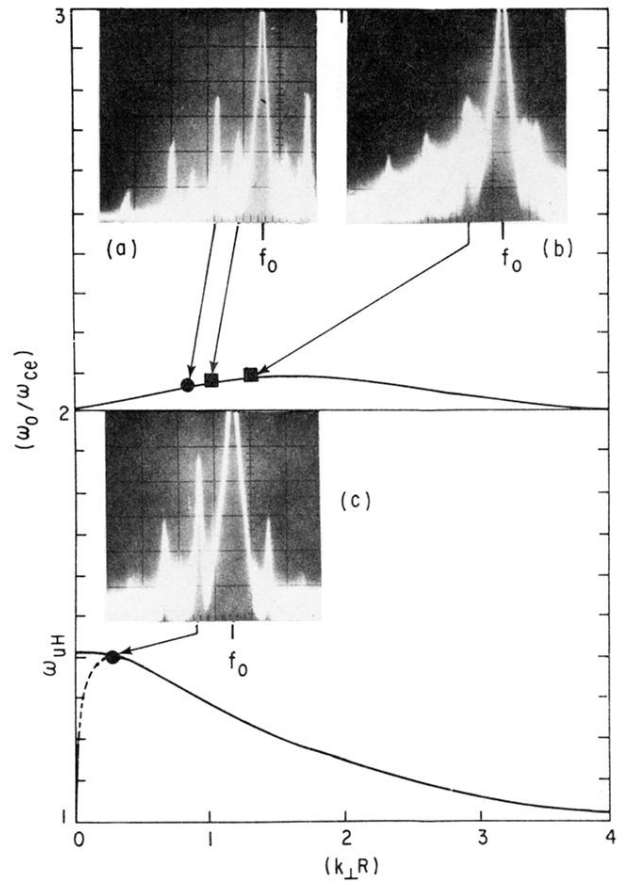


FIG. 1. Dispersion relation for Bernstein waves for $\omega_p = \omega_c$. R is the electron Larmor radius; the dotted line shows effects of finite k_{\parallel} . Insets (a) to (c) show typical decay spectra. The dots are associated with decay into lower hybrid waves, and the squares with ion-acoustic waves. $\omega_0/\omega_c = 2.12$ for spectrum (a), 2.08 for (b), and 1.50 for (c).